# Negative Refractive Index in an Inhomogeneously Broadened Four-Level Inverted-Y Atomic Medium

Nguyen Huy Bang, Nguyen Van Phu, Vu Ngoc Sau, Nguyen Thanh Cong, and Le Van Doai, *Member, IEEE*

***Abstract*—In this paper, we present the study on negative refractive index in an inhomogeneously broadened four-level inverted-Y atomic medium based on electromagnetically induced transparency (EIT). The expressions of the relative permittivity and the relative permeability are derived under Doppler broadening. For this four-level system, we have found two frequency bands of negative refractive index in an optical region corresponding to two EIT windows. The influences of coupling and signal laser fields as well as temperature on frequency bands of negative refractive index are investigated. Our research can be convenient for experimental implementation with real atomic media under different temperatures.**

***Index Terms*—Negative refractive index, electromagnetically induced transparency, doppler broadening.**

## I. Introduction

THE EIT is a quantum interference phenomenon which renders a medium transparent for a weak probe field induced by a strong coupling field [1], [2]. In addition to vanishing absorption, EIT material also possesses a controllable high refractive index, so it has many novel interesting applications such as slow light, lasing without inversion, giant nonlinearity, controllable optical bistability, and so on [2]. Thanks to such unusual properties of the EIT material, it is of great interest to realize a negative refractive index in isotropic atomic gas media. In principle, negative refractive index can be obtained in EIT materials because the magnetic dipole moment can possibly have the same order of magnitude of the electric dipole moment. This allows relative permittivity and relative permeability to be negative simultaneously. Using EIT effect, Oktel *et al.* [3] and Shen *et al.* [4] first proposed a scheme for realization of the negative refractive index in a three-level lambda-type atomic medium. Later, Krowne *et al.* [5] realized a negative refractive index using dressed-state mixed parity transitions of atom. Studies have shown that the generation of negative refractive index based on the EIT effect has the following advantages: first, the negative refractive index is easily obtained in an optical region without absorption; second, the amplitude and the frequency band of the negative refractive index are also easily controlled by external fields.

In addition to the three-level atomic configurations, several other studies on negative index materials have been carried out in four- and five-level atomic systems that can create multiple frequency regions of negative refractive index. For example, Thommen *et al.* [6] and Kastel *et al.* [7] achieved left-handed electromagnetic properties in four-level atomic systems. Liu *et al.* [8] showed that left-handed properties can be electromagnetically induced in $\Lambda$-type four-level scheme on the $Er^{3+}$:$YalO_3$ crystal. Zhang *et al.* [9] proposed a scheme for realization of the negative refractive index in a V-type four-level atomic system. Zhao *et al.* [10]–[12] produced a negative refractive index with vanishing absorption in the four-level system and showed negative refraction can be controlled by an incoherent pump field. Zhang *et al.* [13] showed the negative permittivity and the negative permeability of the medium can be achieved simultaneously in a wider frequency band in a closed V-type four-level dense atomic vapor. Othman *et al.* [14] demonstrated that a negative index of refraction can be achieved over a wide wavelength range with minimal absorption in a five-level atomic system. Very recently, Al–Toki *et al.* [15] studied negative refractive index in a double quantum dot and obtained a high negative refractive index corresponding to neglected absorption under applied electric fields between quantum dot-quantum dot.

However, the above studies on negative refractive index in EIT materials have often ignored Doppler broadening and thus they can only be suitable for ultra-cooled atoms confined in a magneto-optical trap (MOT). In order to be able to apply EIT materials in practice operating under different temperature conditions, Doppler effect has been included in some recent studies on EIT [16]–[23], group velocity of light [24]–[27], pulse propagation [28], [29], Kerr nonlinearity [30]–[34]. It showed that the influence of Doppler broadening on the EIT and related phenomena at room temperature should be considered.

In this work, we present the realization of negative refractive index in a Doppler broadened four-level inverted Y-type atomic medium. This four-level inverted-Y scheme is consisted of two sub-systems $\Lambda + \Xi$, so it can exhibit two transparency windows for the probe laser field [35]. These transparency windows can be manipulated by the intensity and the frequency of the coupling and signal fields. From the physics point of view, this scheme is favorable to generate negative refractive index at two frequency regions corresponding to the two transparency windows and can shift these frequency bands by the control two laser fields.

Manuscript received September 28, 2021; accepted October 8, 2021. Date of publication October 14, 2021; date of current version November 3, 2021. This work was supported by Vietnamese National Foundation of Science and Technology Development (103.03-2019.383). *(Corresponding author: Le Van Doai).*

The authors are with the Department of Physics, Vinh University, Vinh City 460000, Vietnam. (e-mail: bangnh@vinhuni.edu.vn; phunv@vinhuni.edu.vn; sauvn@vinhuni.edu.vn; nhatancong@gmail.com; doailv@vinhuni.edu.vn).

Digital Object Identifier 10.1109/JPHOT.2021.3119985

This work is licensed under a Creative Commons Attribution 4.0 License. For more information, see https://creativecommons.org/licenses/by/4.0/

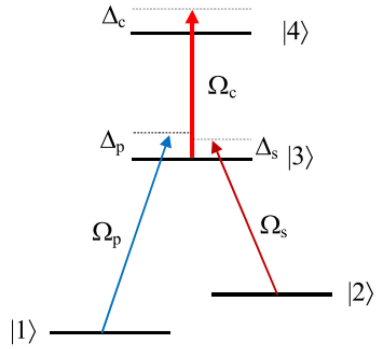


Fig. 1. Four-level inverted-Y atomic system induced by probe, coupling and signal laser fields.

## II. Theoretical Model

A schematic diagram of the four-level inverted-Y atomic system considered in the present work is shown in Fig. 1. The ground states $|1\rangle$ and $|2\rangle$ are coupled with the intermediate excited state $|3\rangle$ by weak probe and strong signal fields, respectively. Meanwhile, a strong coupling field is applied to the transition between the intermediate excited state $|3\rangle$ and the uppermost excited state $|4\rangle$. Thus, this composite system consists of two sub-systems as lambda-type and ladder-type connected by common state $|2\rangle$. The transitions from the two ground states to the intermediate state $|3\rangle$ and from the intermediate state $|3\rangle$ to the uppermost level $|4\rangle$ are electric-dipole allowed. The transition between the two ground states $1\rangle$ and $|2\rangle$ is magnetic-dipole allowed. So, we use the electric-dipole allowed transition $|1\rangle\leftrightarrow|3\rangle$ and the magnetic-dipole allowed transition $|1\rangle\leftrightarrow|2\rangle$ to expect that the negative permittivity and permeability are simultaneously negative for the probe field.

The probe, coupling and signal fields have the frequency detunings $\Delta_p = \omega_p - \omega_{31}$, $\Delta_c = \omega_c - \omega_{43}$ and $\Delta_s = \omega_s - \omega_{32}$, respectively. The Rabi frequencies of the probe, coupling and signal fields are $\Omega_{\rm p} = d_{31}E_p/\hbar$, $\Omega_{\rm c} = d_{42}E_c/\hbar$ and $\Omega_{\rm s} = d_{32}E_s/\hbar$, respectively, where $d_{ij}$ is the electric-dipole matrix elements. We denote $\gamma_{ij}$ are the decay rate of the atomic coherences $\rho_{ij}$.

The master equation describing the dynamical evolution of atoms in laser fields is given by:

$$\dot{\rho} = -\frac{i}{\hbar}[H,\rho] + \Lambda\rho, \tag{1}$$

where $H$ is the total Hamiltonian and $\Lambda\rho$ represents decaying processes.

In dipole and rotating-wave approximations, the density-matrix equations of motion for this four-level system are derived from Eq. (1) as follows:

$$\dot{\rho}_{23} = [-i\Delta_s - \gamma_{32}]\rho_{23} + \frac{i}{2}\Omega_s(\rho_{33}-\rho_{22}) - \frac{i}{2}\Omega_p\rho_{21} - \frac{i}{2}\Omega_c\rho_{24} \tag{2}$$

$$\dot{\rho}_{24} = [-i(\Delta_c+\Delta_c) - \gamma_{42}]\rho_{24} + \frac{i}{2}\Omega_s\rho_{34} - \frac{i}{2}\Omega_c\rho_{23} \tag{3}$$

$$\dot{\rho}_{34} = [-i\Delta_s - \gamma_{43}]\rho_{34} - \frac{i}{2}(\Omega_p\rho_{14} + \Omega_s\rho_{24}) + \frac{i}{2}\Omega_c(\rho_{44}-\rho_{43}) \tag{4}$$

$$\dot{\rho}_{21} = [i(\Delta_P - \Delta_s) - \gamma_{21}]\rho_{21} - \frac{i}{2}\Omega_p\rho_{23} + \frac{i}{2}\Omega_s\rho_{31} \tag{5}$$

$$\dot{\rho}_{31} = [i\Delta_p - \gamma_{31}]\rho_{31} - \frac{i}{2}\Omega_p(\rho_{33}-\rho_{11}) + \frac{i}{2}\Omega_s\rho_{21} + \frac{i}{2}\Omega_c\rho_{41} \tag{6}$$

$$\dot{\rho}_{41} = [i(\Delta_p+\Delta_c) - \gamma_{41}]\rho_{41} - \frac{i}{2}\Omega_p\rho_{43} + \frac{i}{2}\Omega_c\rho_{31} \tag{7}$$

Now we need to find the solutions of density matrix elements $\rho_{31}$ and $\rho_{21}$ that related to the electric and magnetic polarizabilities of the atom for the probe field, by solving the density matrix equations (2)–(7) under the steady-state condition. We assume that the coupling laser field ($\Omega_{\rm c}$) and the signal laser field ($\Omega_{\rm s}$) are much stronger than the probe laser field ($\Omega_{\rm p}$) and that the atoms initially populate in the ground state $|1\rangle$, i.e., $\rho_{11} = 1$, $\rho_{22} = \rho_{33} = \rho_{44} = 0$. Under these assumptions, the expressions of $\rho_{31}$ and $\rho_{21}$ are found below:

$$\rho_{31} = \frac{i\Omega_p/2}{\gamma_{31} - i\Delta_p + \frac{\Omega_s^2/4}{\gamma_{21}-i(\Delta_p-\Delta_s)} + \frac{\Omega_c^2/4}{\gamma_{41}-i(\Delta_p+\Delta_c)}} \tag{8}$$

$$\rho_{21} = -\frac{\Omega_p/2}{\gamma_{31} - i\Delta_p + \frac{\Omega_s^2/4}{\gamma_{21}-i(\Delta_p-\Delta_s)} + \frac{\Omega_c^2/4}{\gamma_{41}-i(\Delta_p+\Delta_c)}} \times \frac{\Omega_s/2}{\gamma_{21} - i(\Delta_p-\Delta_s)} \tag{9}$$

Thus, the expressions for the macroscopic electric- and magnetic-polarizabilities of the atomic medium to the probe filed are determined by [8]–[12]:

$$\alpha_e = \frac{2Nd_{31}\rho_{31}}{\varepsilon_0 E_p} \equiv \frac{2Nd_{31}^2\rho_{31}}{\varepsilon_0\hbar\Omega_p} \tag{10}$$

$$\alpha_m = \frac{2N\mu_0 m_{21}\rho_{21}}{B_p} \equiv \frac{2Nc\mu_0 m_{21}d_{31}\rho_{21}}{\hbar\Omega_p} \tag{11}$$

here we used $E_p = \hbar\Omega_p/d_{31}$ and $E_p/B_p = c$; $d_{31}$ and $m_{21}$ are respectively the electric and magnetic dipole matrix elements, $\varepsilon_0$ and $\mu_0$ denote the permittivity and the permeability of free vacuum, respectively and $N$ denotes the atomic density of the vapor.

The above calculations were performed with the atoms at rest. However, for atoms moving with thermal velocities at room temperature we need to include the Doppler effect in the expressions of the electric- and magnetic-polarizabilities. In the experiment, to eliminate the first-order Doppler effect for this four-level configuration, the probe and signal fields are usually arranged to propagate in the same direction into the atomic medium, while the coupling field is counter-propagating with the probe field [30]. In this arrangement, when an atom moves with velocity $v$ in the direction of the probe field, it will see the frequencies of the probe, coupling and signal fields shifted by $\omega_p + (v/c)\omega_p$,

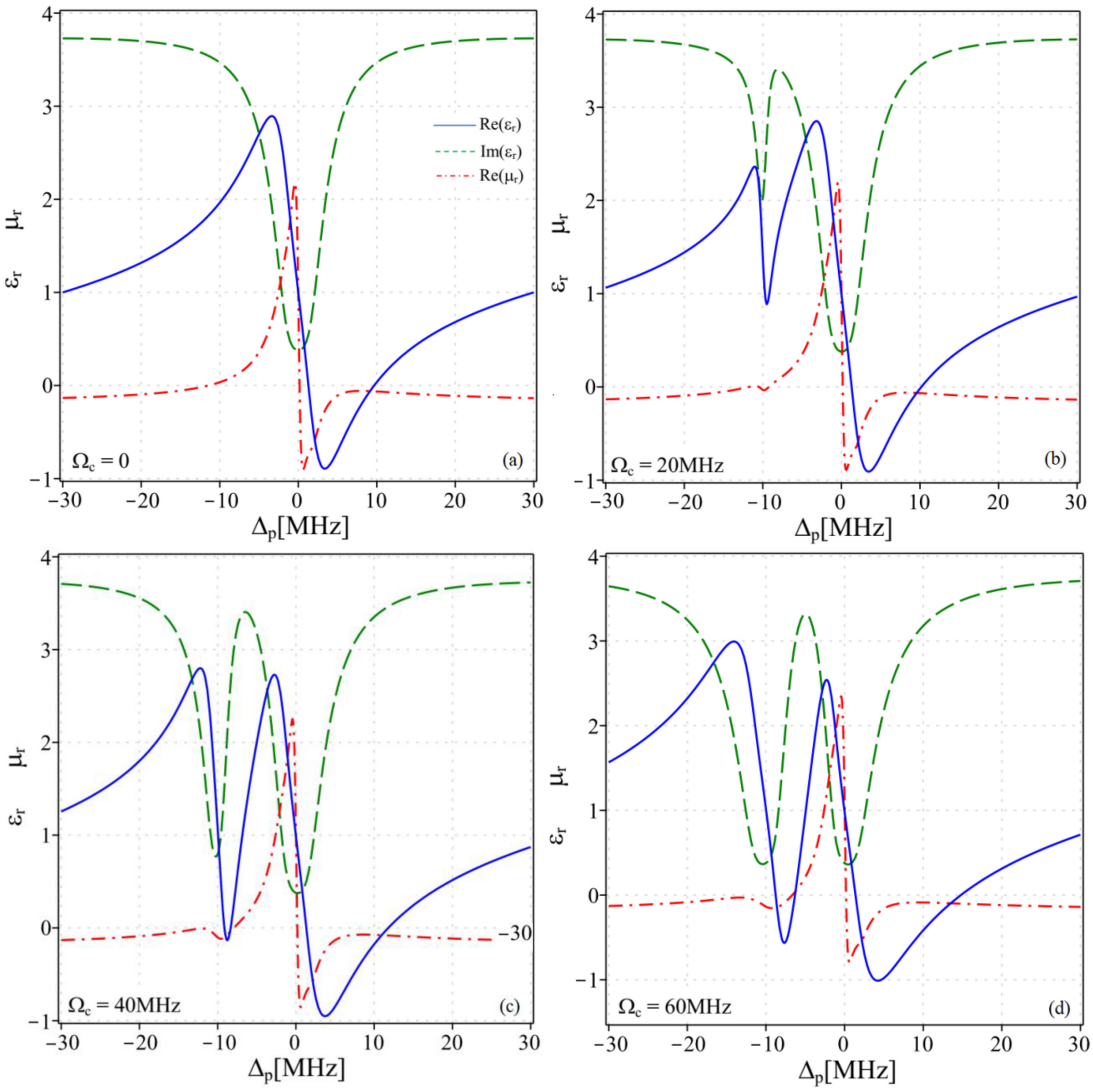


Fig. 2. Real parts of relative permittivity ($\varepsilon_r$) and relative permeability ($\mu_r$) as a function of probe laser detuning for different values of coupling Rabi frequency: (a) $\Omega_c = 0$, (b) $\Omega_c = 20$ MHz, (c) $\Omega_c = 40$ MHz and (d) $\Omega_c = 60$ MHz. Other parameters are scaled as $\Delta_c = 10$ MHz, $\Delta_s = 0$, $\Omega_s = 60$ MHz and T = 340 K.

$\omega_c - (v/c)\omega_c$ and $\omega_s + (v/c)\omega_s$ respectively. Thus, the frequency detunings of the probe and coupling laser beams are also changed to be $\Delta_p \to \Delta_p + (v/c)\omega_p$, $\Delta_c \to \Delta_c - (v/c)\omega_c$ and $\Delta_s \to \Delta_s + (v/c)\omega_s$, respectively. Considering the atoms moving along the axis of the laser beams, then the atomic velocity distribution follows the Maxwell distribution:

$$dN(v) = \frac{N_0}{u\sqrt{\pi}} e^{-v^2/u^2} dv \tag{12}$$

where $u = \sqrt{2k_B T/m}$ with $m$ being the mass of an atom, $k_B$ is Boltzmann's constant and $T$ is the absolute temperature.

In this way, the Doppler effect can be included in the expressions of the electric- and magnetic-polarizabilities as follows:

$$\alpha_e(v)dv = \frac{id_{31}^2}{\varepsilon_0 \hbar u\sqrt{\pi}} \frac{N_0 e^{(-\frac{v^2}{u^2})} dv}{A} dv \tag{13}$$

$$\alpha_m(v)dv = -\frac{c\mu_0 m_{21} d_{31}}{\hbar u\sqrt{\pi}} \frac{\Omega_s/2}{\gamma_{21} - i(\Delta_p - \Delta_s) - i\frac{(\omega_p - \omega_s)v}{c}}$$

$$\times \frac{N_0 e^{(-\frac{v^2}{u^2})} dv}{A} dv \tag{14}$$

$$A = \gamma_{31} - i\Delta_p - i\frac{\omega_p}{c}v + \frac{\Omega_s^2/4}{\gamma_{21} - i(\Delta_p - \Delta_s) - i\frac{(\omega_p - \omega_c)v}{c}} + \frac{\Omega_c^2/4}{\gamma_{41} - i(\Delta_p + \Delta_c) + i\frac{(\omega_p - \omega_c)v}{c}} \tag{15}$$

After integrating with respect to $v$ from -∞ to +∞, the expressions of the electric- and magnetic-polarizabilities in the presence of Doppler broadening as:

$$\alpha_e(D) = \frac{iN_0 d_{21}^2 \sqrt{\pi}}{\varepsilon_0 \hbar \left(\frac{\omega_p u}{c}\right)} \left[e^{a^2}\left(1 - erf(a)\right)\right] \tag{16}$$

$$\alpha_m(D) = -\frac{N_0 c\mu_0 m_{21} d_{31}\sqrt{\pi}}{\hbar \left(\frac{\omega_p u}{c}\right)} \frac{\Omega_s/2}{\gamma_{21} - i(\Delta_p - \Delta_s)}$$

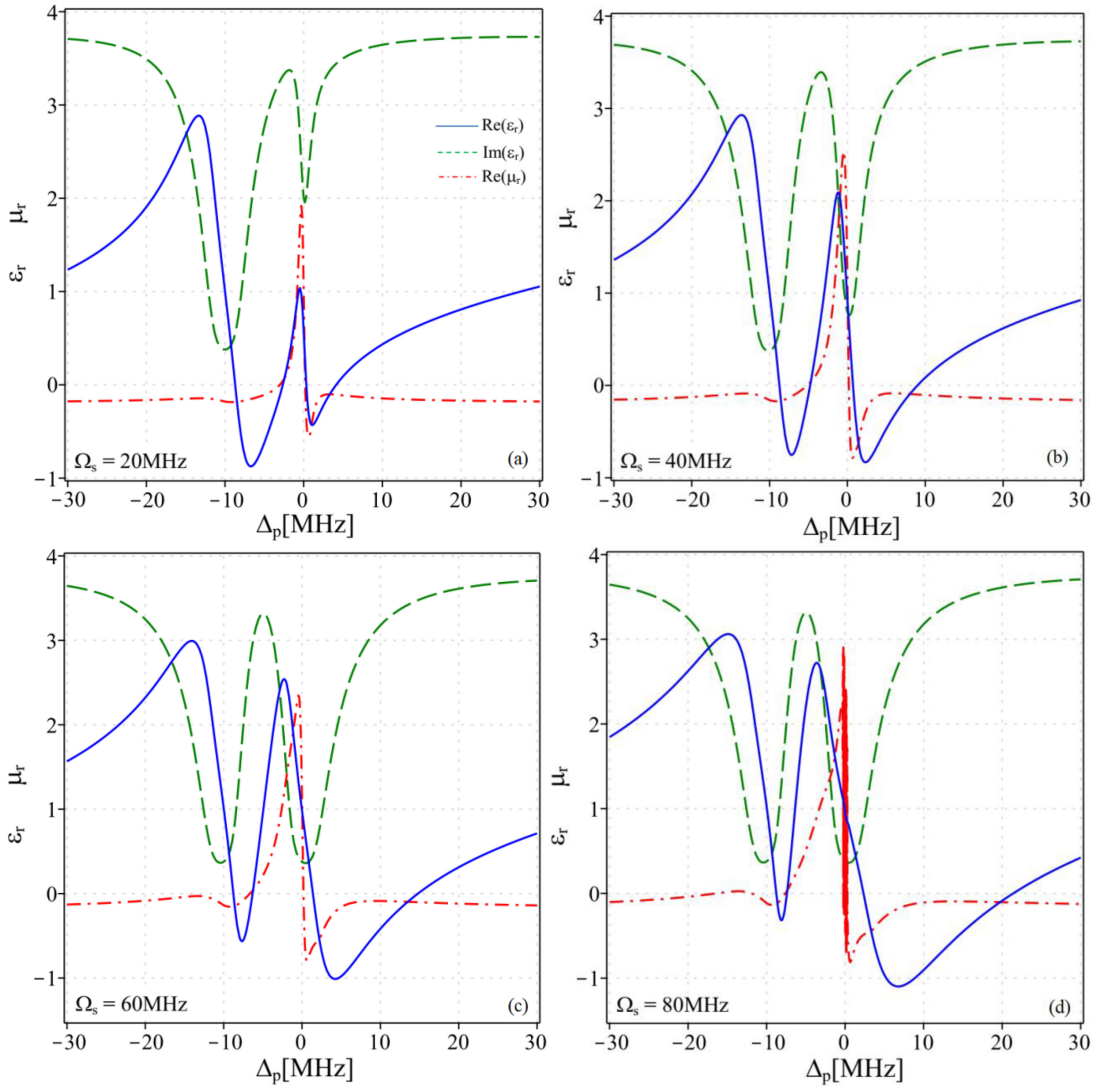


Fig. 3. Real parts of relative permittivity ($\varepsilon_r$) and relative permeability ($\mu_r$) as a function of probe laser detuning for different values of signal laser intensity: (a) $\Omega_s = 20$ MHz, (b) $\Omega_s = 40$ MHz, (c) $\Omega_s = 60$ MHz and (d) $\Omega_s = 80$ MHz. Other parameters are scaled as $\Delta_c = 10$ MHz, $\Delta_s = 0$, $\Omega_c = 60$ MHz and T = 340 K.

$$\times \left[e^{a^2}\left(1 - erf(a)\right)\right] \tag{17}$$

where

$$a = \frac{c}{\omega_p u} \times \left(\gamma_{31} - i\Delta_p + \frac{\Omega_s^2/4}{\gamma_{21} - i(\Delta_p - \Delta_s)} + \frac{\Omega_c^2/4}{\gamma_{41} - i(\Delta_p + \Delta_c)}\right) \tag{18}$$

and *erf*(*a*) is the error function.

Taking into account the local field effect, the electric- and magnetic- susceptibilities of the atomic medium can obtain from Clausius-Mossotti relations [36] as follows:

$$\chi_e = \frac{\alpha_e(D)}{1 - \frac{\alpha_e(D)}{3}} \tag{19}$$

$$\chi_m = \frac{\alpha_m(D)}{1 - \frac{\alpha_m(D)}{3}} \tag{20}$$

The relative permittivity and the relative permeability of the atomic medium reads

$$\varepsilon_r = 1 + \chi_e = \frac{1 + 2/3\alpha_e(D)}{1 - 1/3\alpha_e(D)} \tag{21}$$

$$\mu_r = 1 + \chi_m = \frac{1 + 2/3\alpha_m(D)}{1 - 1/3\alpha_m(D)} \tag{22}$$

In negative index material, the expression of refractive refraction is defined by

$$n = -\sqrt{\varepsilon_r \mu_r} \tag{23}$$

## III. Results and Discussion

For specificity, we realize negative refractive index in $^{87}$Rb atomic vapor [37], where level $|1\rangle$ is the hyperfine level F = 1 of

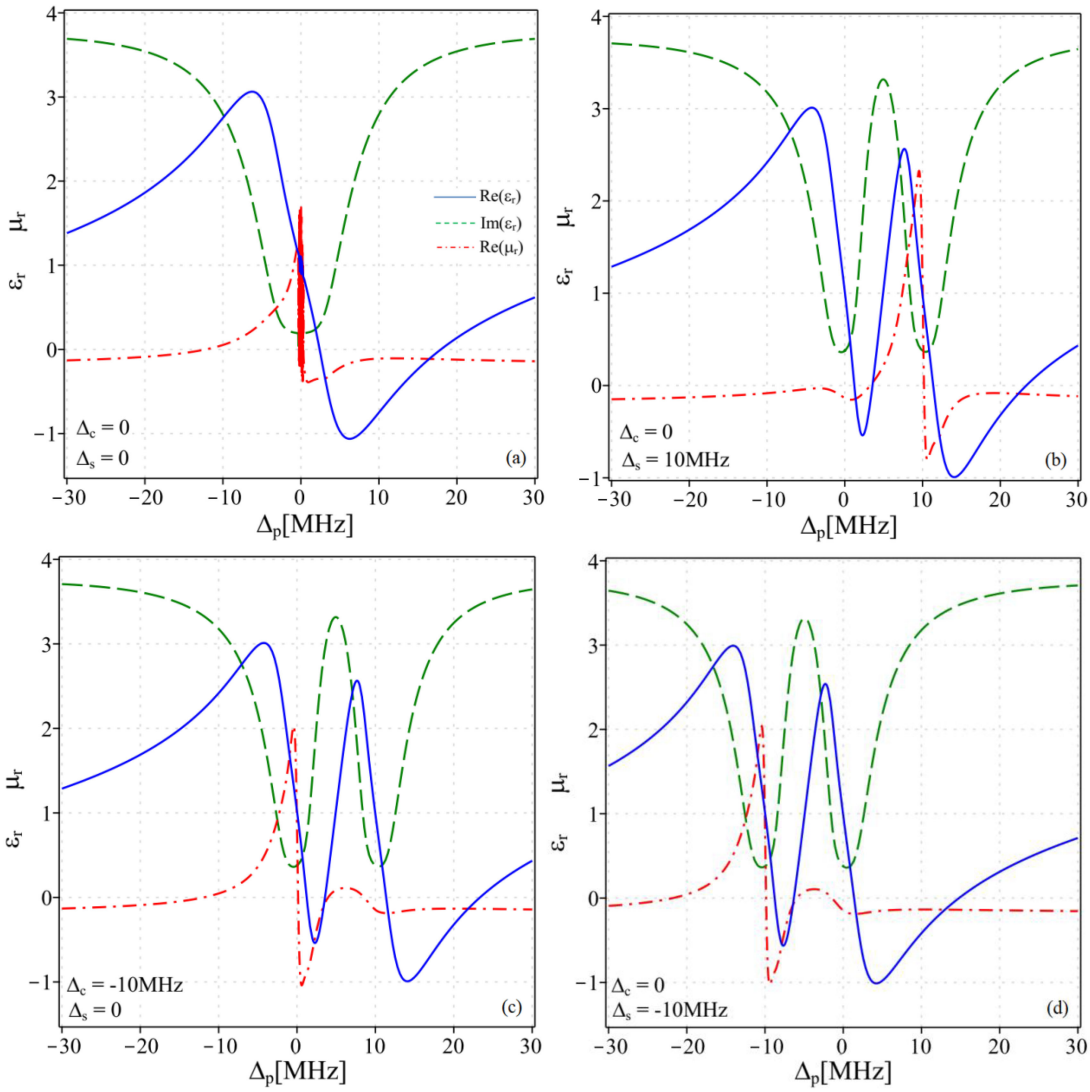


Fig. 4. Real parts of relative permittivity ($\varepsilon_r$) and relative permeability ($\mu_r$) as a function of probe laser detuning for different values of coupling and signal laser detunings: (a) $\Delta_c = \Delta_s = 0$, (b) $\Delta_c = 0$ and $\Delta_s = 10$ MHz, (c) $\Delta_c = -10$ MHz and $\Delta_s = 0$, and (d) $\Delta_c = 0$ and $\Delta_s = -10$ MHz. Other parameters are scaled as $\Omega_c = \Omega_s = 60$ MHz and T = 340 K.

the ground state $5S_{1/2}$; level $|2\rangle$ is the hyperfine level F = 2 of the ground state $5S_{1/2}$; level $|3\rangle$ is the hyperfine level F′ = 1 of the state $5P_{3/2}$; and level $|4\rangle$ is the hyperfine level F″ = 1 of the state $5D_{5/2}$. The corresponding decay rates are $\gamma_{31} = 6.1$ MHz, $\gamma_{32} = 5.9$ MHz and $\gamma_{43} = 0.5$ MHz; $N = 10^{25}$ atoms/m$^3$; $d_{31} = 1.6 \times 10^{-29}$ C.m, $m_{21} = 7.26 \times 10^{-23}$ A.m$^2$.

Firstly, we fix the parameters of signal laser field at $\Delta_s = 0$ and $\Omega_s = 60$ MHz and consider the dependence of relative permittivity ($\varepsilon_r$) and relative permeability ($\mu_r$) on the coupling laser intensity. In Fig. 2 we have presented the graphs of the relative permittivity and the relative permeability at different values of coupling Rabi frequency $\Omega_c = 20$ MHz (a), $\Omega_c = 40$ MHz (b), $\Omega_c = 60$ MHz (c) and $\Omega_c = 80$ MHz (d). From Fig. 2(a), it shows that when $\Omega_c = 0$ (without coupling laser), only one EIT window induced by the signal laser field appears at position $\Delta_p = 0$. At the same time, we also find that the real parts of relative permittivity ($\varepsilon_r$) and the relative permeability ($\mu_r$) are simultaneously negative in the frequency detuning range [2 MHz, 9 MHz]. From Fig. 2(b) with $\Omega_c = 20$ MHz and $\Delta_c = 10$ MHz, a second EIT window induced by the coupling laser appears at position $\Delta_p = -10$ MHz, however, negative refractive index has not appeared at this EIT window yet. In Fig. 2(c) with $\Omega_c = 40$ MHz, the EIT window at position $\Delta_p = -10$ MHz becomes clearer and negative refractive index begins to appear at this EIT window. When $\Omega_c = 60$ MHz (Fig. 2d), the two EIT windows have similar depth and width, the real parts of relative permittivity and the relative permeability are simultaneously negative in two ranges [−8 MHz, −6 MHz] and [2 MHz, 13 MHz].

Next, we fix the parameters of the coupling laser at $\Omega_c = 60$ MHz and $\Delta_c = 10$ MHz and study the dependence of the relative permittivity and the relative permeability on the signal

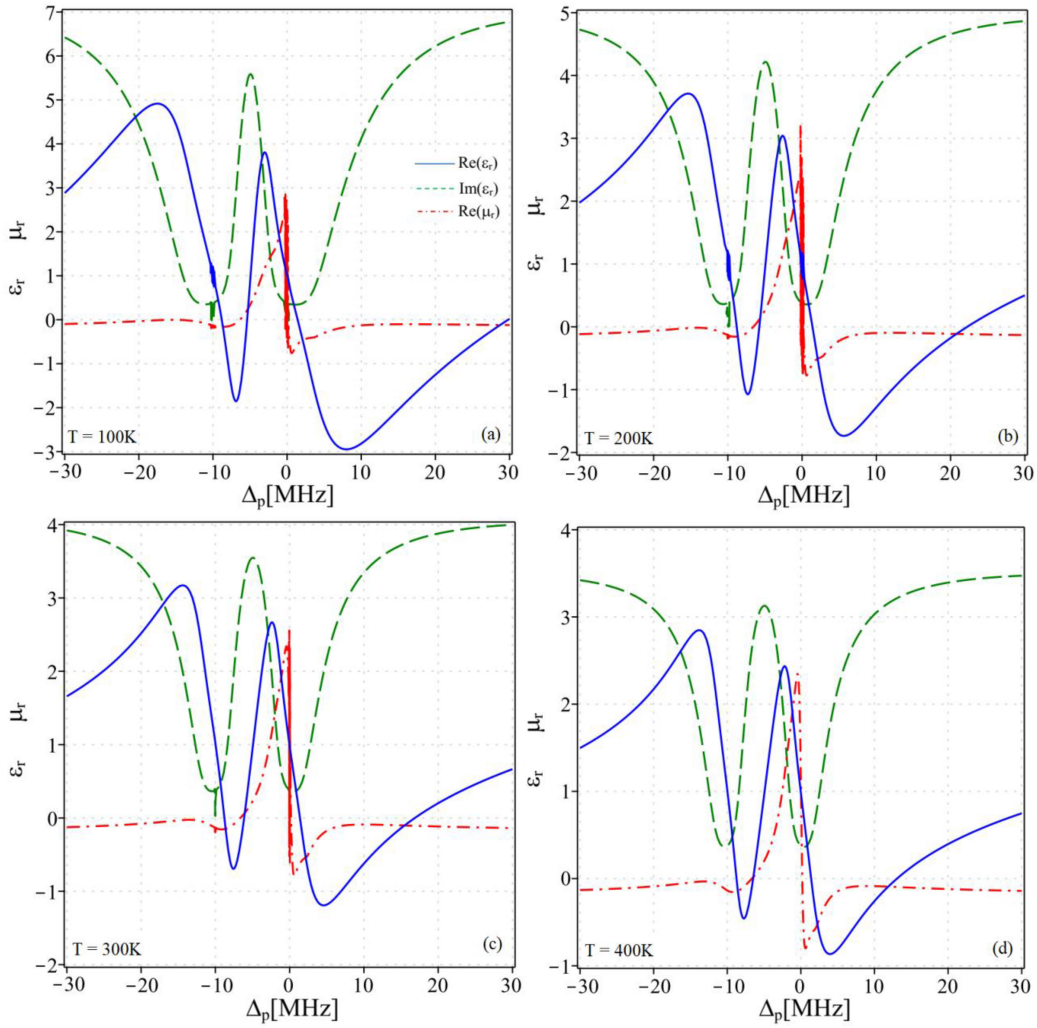


Fig. 5. Real parts of relative permittivity ($\varepsilon_r$) and relative permeability ($\mu_r$) as a function of probe laser detuning for different values of temperature: (a) T = 100 K, (b) T = 200 K, (c) T = 300 K and (d) T = 400 K. Other parameters are scaled as $\Omega_c = \Omega_s = 60$ MHz, $\Delta_c = 10$ MHz and $\Delta_s = 0$.

laser intensity. From Fig. 3(a) with $\Omega_s = 20$ MHz, the negative refractive index appears in two ranges [−8 MHz, −4 MHz] and [0, 4 MHz] corresponding to two EIT windows at $\Delta_p = -10$ MHz and $\Delta_p = 0$, however, the frequency band and the amplitude of negative refractive index corresponding to the EIT window at $\Delta_p = 0$ are smaller than those at $\Delta_p = -10$ MHz. As the intensity of the laser signal is increased, the frequency range and the amplitude of the negative refractive index corresponding to the EIT window at $\Delta_p = 0$ are also increased (see Figs. 3(b)–(d)). Meanwhile, the frequency range of the negative refractive index corresponding to the EIT window at $\Delta_p = -10$ MHz becomes narrower as the signal laser intensity increases. In particular, in Fig. 3(d) with $\Omega_s = 80$ MHz, two ranges of negative refractive index corresponding to the EIT windows at $\Delta_p = -10$ MHz and $\Delta_p = 0$ are now [−8 MHz, −7 MHz] and [4 MHz, 20 MHz].

In Fig. 4 we consider the influence of laser frequency on the frequency band of negative refractive index. The investigation in Fig. 4(a) with $\Delta_c = \Delta_s = 0$ shows that the two EIT windows (induced by the coupling and signal fields) overlap, so that the depth and the width of this dual EIT window are larger than that in Fig. 3(c). As a consequence, the frequency band of negative refractive index is wider than that in Fig. 3(c). In this case, the negative refractive index occurs in range [3 MHz, 17 MHz]. In Fig. 4(b) we have chosen $\Delta_c = 0$ and $\Delta_s = 10$ MHz, so that the EIT window induced by the coupling laser is located at $\Delta_p = 0$, while the EIT window at $\Delta_p = 10$ MHz is induced by the signal laser. Thus, the position of the EIT windows has been shifted on the axis $\Delta_p$, and hence the frequency bands of negative refractive index are also shifted on the axis $\Delta_p$ by the same amount. In this case, the negative refractive index appears in two ranges [2 MHz, 4 MHz] and [12 MHz, 24 MHz]. In Fig. 4(c) with $\Delta_c = -10$ MHz and $\Delta_s = 0$, the position of the EIT window induced by the coupling laser is located at $\Delta_p = 10$ MHz, while the EIT window induced by the signal laser is still located at $\Delta_p = 0$, so that the two ranges of negative refractive index are now [2 MHz, 4 MHz] and [12 MHz, 24 MHz]. In Fig. 4(d), we have chosen $\Delta_c = 0$ and $\Delta_s = -10$ MHz, the positions of the EIT windows induced by the coupling and signal lasers are located at $\Delta_p = 0$ and $\Delta_p = -10$ MHz, respectively. In this case, the ranges of negative refractive index are at [−9 MHz,

−6 MHz] and [2 MHz, 15 MHz]. Thus, we can shift the bands of negative refractive index by varying the frequency detuning of the coupling and/or signal lasers.

Finally, in Fig. 5 we investigate the influence of temperature (Doppler width) on the negative refractive index by plotting the relative permittivity and relative permeability at different temperatures T = 100 K (a), T = 200 K (b), T = 300 (c) and T = 400 (d) when fixed the laser parameters at $\Omega_c = \Omega_s =$ 60 MHz, $\Delta_c = 10$ MHz and $\Delta_s = 0$. We can see that the amplitude and the frequency bands of negative refractive index decrease markedly as the temperature of the medium increases. It is because increasing temperature reduces the efficiency of EIT [19].

## IV. Conclusion

Negative refractive index in an inhomogeneously broadened four-level inverted-Y atomic gas medium is achieved in two optical frequency bands. The frequency bands of negative refractive index are controlled by the intensity and the frequency of coupling and signal laser fields. The frequency width of the negative refractive index can be extended with increasing laser intensity, while its frequency band can be shifted by changing the laser frequency. The amplitude and the frequency bands of negative refractive index are also significantly changed with an increase in atomic temperature. Our research can be convenient for experimental implementation with real atomic media under different temperature conditions.

## References


[1] K. J. Boller, A. Imamoglu, and S. E. Harris, "Observation of electromagnetically induced transparency," *Phys. Rev. Lett.*, vol. 66, 1991, Art. no. 2593.

[2] N. H. Bang, L. V. Doai, and D. X. Khoa, "Controllable optical properties of multiple electromagnetically induced transparency in gaseous atomic media," *Commun. Phys.*, vol. 28, pp. 1–33, 2019.

[3] M. O. Oktel and O. E. Mustecaplioglu, "Electromagnetically induced left-handedness in a dense gas of three-level atoms," *Phys. Rev. A*, vol. 70, 2004, Art. no. 053806.

[4] J. Q. Shen, Z. C. Ruan, and S. He, "How to realize a negative refractive index material at the atomic level in an optical frequency range," *J. Zhejiang Univ. Sci.*, vol. 5, p. 1322, 2004.

[5] C. M. Krowne and J. Q. Shen, "Dressed-state mixed-parity transitions for realizing negative refractive index," *Phys. Rev. A*, vol. 79, pp. 1–11, 2009.

[6] Q. Thommen and P. Mandel, "Electromagnetically induced left handedness in optically excited four-level atomic media," *Phys. Rev. Lett.*, vol. 96, 2006, Art. no. 053601.

[7] J. Kastel, M. Fleischhauer, S. F. Yelin, and R. L. Walsworth, "Tunable negative refraction without absorption via electromagnetically induced chirality," *Phys. Rev. Lett.*, vol. 99, 2007, Art. no. 073602.

[8] C. Liu, J. Zhang, J. Liu, and G. Jin, "The electromagnetically induced negative refractive index in the Er3+: YAlO3 crystal," *J. Phys. B: At., Mol. Opt. Phys.*, vol. 42, 2009, Art. no. 095402.

[9] H. J. Zhang, Y. P. Niu, and S. Q. Gong, "Electromagnetically induced negative refractive index in a V-type four-level atomic system," *Phys. Lett. A*, vol. 363, 2007, Art. no. 497.

[10] S. C. Zhao, Z. D. Liu, and Q. X. Wu, "Left-handedness without absorption in the four-level Y-type atomic medium," *Chin. Phys. B*, vol. 19, 2010, Art. no. 014211.

[11] S. C. Zhao, Z. D. Liu, and Q. X. Wu, "Negative refraction without absorption via both coherent and incoherent fields in a four-level left-handed atomic system," *Opt. Commun.*, vol. 283, pp. 3301–3304, 2010.

[12] S. C. Zhao, Z. D. Liu, and Q. X. Wu, "Zero absorption and a large negative refractive index in a left-handed four-level atomic medium," *J. Phys. B: At., Mol. Opt. Phys.*, vol. 43, 2010, Art. no. 045505.

[13] Z. Q. Zhang, Z. D. Liu, S. C. Zhao, J. Zheng, Y. F. Ji, and N. Liu, "Negative refractive index in a four-level atomic system," *Chin. Phys. B*, vol. 20, 2011, Art. no. 124202.

[14] A. Othman and D. Yevick, "Enhanced negative refractive index control in a 5-level system," *J. Mod. Opt.*, vol. 64, pp. 1208–1214, 2016.

[15] H. G. Al–Toki and A. H. Al–Khursan, "Negative refraction in the double quantum dot system," *Opt. Quant. Elec.*, vol. 52, 2020, Art. no. 467.

[16] Y. Q. Li and M. Xiao, "Electromagnetically induced transparency in ladder-type inhomogeneously broadened media: Theory and experiment," *Phys. Rev. A.*, vol. 51, pp. 576–584, 1995.

[17] L. Zhang, F. Zhou, Y. Niu, J. Zhang, and S. Gong, "The effect of doppler broadening on dispersive and absorptive properties in atomic systems with two-photon interference," *Opt. Commun.*, vol. 284, pp. 5697–5701, 2011.

[18] S. Mitra, S. Dey, M. M. Hossain, P. N. Ghosh, and B. Ray, "Temperature and magnetic field effects on the coherent and saturating resonances in Λ- and V-type systems for the $^{85}$Rb-D2 transition," *J. Phys. B: At., Mol. Opt. Phys.*, vol. 46, 2013, Art. no. 075002.

[19] D. X. Khoa, P. V. Trong, L. V. Doai, and N. H. Bang, "Electromagnetically induced transparency in a five-level cascade system under doppler broadening: An analytical approach," *Phys, Scr.* vol. 91, 2016, Art. no. 035401.

[20] A. Ghosh, K. Islam, D. Bhattacharyya, and A. Bandyopadhyay, "Revisiting the four-level inverted-Y system under both Doppler-free and doppler broadened conditions: An analytical approach," *J. Phys. B: At., Mol. Opt. Phys.*, vol. 49, 2016, Art. no. 195401.

[21] P. Kaur, V. Bharti, and A. Wasan, "Optical properties of an inhomogeneously broadened multilevel V-system in the weak and strong probe regimes," *Ind. J. Phys.*, vol. 91, pp. 1115–1125, 2017.

[22] D. X. Khoa, L. C. Trung, P. V. Thuan, L. V. Doai, and N. H. Bang, "Measurement of dispersive profile of a multi-window EIT spectrum in a Doppler-broadened atomic medium," *J. Opt. Soc. Amer. B*, vol. 34, pp. 1255–1263, 2017.

[23] G. Zhang, Q. Tao, Z. Zhao, and Z. Ren, "Effect of thermal motion on the phenomenon of electromagnetically induced transparency," *Optik*, vol. 138, pp. 153–159, 2017.

[24] H. Ali, Ziauddin and I. Ahmad, "The effect of Kerr nonlinearity and doppler broadening on slow light propagation," *Laser Phys.*, vol. 24, 2014, Art. no. 025201.

[25] V. Bharti and V. Natarajan, "Sub- and super-luminal light propagation using a rydberg state," *Opt. Commun.*, vol. 392, pp. 180–184, 2017.

[26] O. Katz and O. Firstenberg, "Light storage for one second in room-temperature alkali vapor," *Natute Comm.*, vol. 9, 2018, Art. no. 2047.

[27] N. T. Anh, L. V. Doai, D. H. Son, and N. H. Bang, "Manipulating multi-frequency light in a five-level cascade EIT medium under doppler broadening," *Optik*, vol. 171, pp. 721–727, 2018.

[28] L. Li and G. Huang, "Linear and nonlinear light propagations in a Doppler-broadened medium via electromagnetically induced transparency," *Phys. Rev. A*, vol. 82, 2010, Art. no. 023809.

[29] D. X. Khoa, H. M. Dong, L. V. Doai, and N. H. Bang, "Propagation of laser pulse in a three-level cascade inhomogeneously broadened medium under electromagnetically induced transparency conditions," *Optik*, vol. 131, pp. 497–505, 2017.

[30] H. Wang, D. Goorskey, and M. Xiao, "Enhanced Kerr nonlinearity via atomic coherence in a three-level atomic system," *Phys. Rev. Lett.*, vol. 87, 2001, Art. no. 073601.

[31] J. Sheng, X. Yang, H. Wu, and M. Xiao, "Modified self-Kerr-nonlinearity in a four-level N-type atomic system," *Phys. Rev. A*, vol. 84, 2011, Art. no. 053820.

[32] N. H. Bang, D. X. Khoa, D. H. Son, and L. V. Doai, "Effect of doppler broadening on giant self-Kerr nonlinearity in a five-level ladder-type system," *J. Opt. Soc. Am. B*, vol. 36, 2019, Art. no. 3151.

[33] L. V. Doai, "Giant cross-Kerr nonlinearity in a six-level inhomogeneously broadened atomic medium," *J. Phys. B: At., Mol. Opt. Phys.*, vol. 52, 2019, Art. no. 225501.

[34] N. H. Bang, D. X. Khoa, and L. V. Doai, "Controlling self-Kerr nonlinearity with an external magnetic field in a degenerate two-level inhomogeneously broadened medium," *Phys. Lett. A*, vol. 384, 2020, Art. no. 126234.

[35] A. Joshi and M. Xiao, "Electromagnetically induced transparency and its dispersion properties in a four-level inverted-Y atomic system," *Phys. Lett. A*, vol. 317, 2003, Art. no. 370.

[36] J. D. Jackson, *Classical Electrodynamics*, 3rd ed., Hoboken, NJ, USA: Wiley, 2001, Chap. 4, pp. 159–162.

[37] Daniel Adam Steck, $^{87}$Rb D Line Data. 2021, [Online]. Available: http://steck.us/alkalidata